

Cite this: *Anal. Methods*, 2017, 9, 402

## Monitoring carnosine uptake by RAW 264.7 macrophage cells using microchip electrophoresis with fluorescence detection

Claudia G. Fresta,<sup>ab</sup> Michael L. Hogard,<sup>†ac</sup> Giuseppe Caruso,<sup>†ab</sup> Elton E. Melo Costa,<sup>ad</sup> Giuseppe Lazzarino<sup>e</sup> and Susan M. Lunte<sup>\*abc</sup>

Carnosine, a dipeptide found in a variety of tissues, is believed to possess antioxidant properties. It serves as a scavenger of reactive nitrogen and oxygen species (RNOS), which are important stress mediators of pro-inflammatory conditions and can lead to macrophage activation. In this study, intracellular concentrations of carnosine in murine RAW 264.7 macrophage cells were determined using microchip electrophoresis with laser-induced fluorescence detection following derivatization with naphthalene-2,3-dicarboxaldehyde and cyanide. The method was linear from 25 nM to 5  $\mu$ M with a limit of detection in cell lysate samples of 65 nM. Using the method of standard additions, the basal intracellular content of carnosine in macrophage cells was determined to be  $0.079 \pm 0.02$  nmol per  $10^6$  cells. The uptake of carnosine by these cells was then investigated under both physiological and pro-inflammatory conditions. There was a 2.8-fold increase in carnosine uptake for macrophages exposed to lipopolysaccharides and interferon- $\gamma$  prior to incubation, compared to the controls. This suggests that macrophages may use carnosine uptake as a defense mechanism under pro-inflammatory conditions. Future studies will investigate the role of the carnosine transporter in carnosine uptake and its possible correlation with cell morphological changes observed after stimulation.

Received 3rd November 2016  
Accepted 13th December 2016

DOI: 10.1039/c6ay03009b

[www.rsc.org/methods](http://www.rsc.org/methods)

### Introduction

Carnosine is an endogenous dipeptide composed of  $\beta$ -alanine and L-histidine that is synthesized by the enzyme carnosine synthase. This dipeptide is naturally present in several mammalian tissues,<sup>1</sup> with the highest concentrations observed in skeletal and cardiac muscle as well as in the brain.<sup>2–4</sup> Furthermore, *in vivo* studies have shown that immune tissues, such as the spleen, and biological fluids (*e.g.*, plasma and cerebrospinal fluid) contain smaller amounts of carnosine.<sup>5</sup> There are a number of observations that suggest that carnosine exhibits antioxidant properties and protects cells against free radicals, scavenging both reactive nitrogen and oxygen species (RNOS).<sup>6</sup> These species are widely recognized as important stress mediators of pro-inflammatory conditions.<sup>7</sup> Both *in vitro* and *in vivo* experiments have shown the ability of carnosine to

prevent oxidative stress-induced pathologies such as atherosclerosis,<sup>8</sup> diabetic complications,<sup>9</sup> ischemia-reperfusion,<sup>10</sup> and neurodegeneration<sup>11</sup> due to its antioxidant, chelating, and anti-glycation functions.<sup>1</sup> In addition, carnosine is involved in the regulation of macrophage function<sup>12</sup> and has been shown to increase the phagocytotic activity of peritoneal macrophages by interacting with specific receptors localized on the plasma membranes of these cells.<sup>13</sup> Macrophages are the primary cell type activated under pro-inflammatory conditions as a part of the immune response.<sup>14</sup> Activation leads to an increased expression of inducible nitric oxide synthase (iNOS) coupled to the production of higher amounts of RNOS.<sup>15</sup>

Microchip electrophoresis (ME) has been used extensively for bulk cell lysate analysis.<sup>16–21</sup> Due to the short length of microfluidic channels and the high field strengths applied, separations occur quickly and with minimal sample dilution in the background electrolyte. The short timescales characteristic of ME (30–180 seconds) also allows for higher throughput compared to other separation methods, such as conventional capillary electrophoresis or liquid chromatography. Additionally, ME requires very small (micro- or nanoliter) volumes of sample, which can be especially important for the analysis of precious biological samples because it reduces the amount of sample that is consumed and the associated analysis costs. When examining bulk cell lysate samples, this also makes it possible to conduct several analyses on the same

<sup>a</sup>Ralph N. Adams Institute for Bioanalytical Chemistry, University of Kansas, Lawrence, Kansas, USA. E-mail: slunte@ku.edu; Fax: +1-785-864-1916; Tel: +1-785-864-3811

<sup>b</sup>Department of Pharmaceutical Chemistry, University of Kansas, Lawrence, Kansas, USA

<sup>c</sup>Department of Chemistry, University of Kansas, Lawrence, Kansas, USA

<sup>d</sup>Institute of Chemistry and Biotechnology, Federal University of Alagoas, Alagoas, Brazil

<sup>e</sup>Department of Biomedical and Biotechnological Sciences, Division of Medical Biochemistry, University of Catania, Italy

<sup>†</sup> These authors contributed equally to this work.

batch of cells in order to ensure the reproducibility of the results. ME pairs well with biological matrixes with high conductivity (*e.g.* bulk cell lysates) due to the nature of the separation. Other common analytical methods, such as liquid chromatography-tandem mass spectrometry (LC-MS), often require extensive sample preparation in order to desalt these samples before small molecules can be separated from the biological matrix.<sup>22</sup> Finally, ME can easily be combined with a sensitive detection method such as laser-induced fluorescence (ME-LIF) to detect compounds at physiologically relevant concentrations.

Naphthalene-2,3-dicarboxaldehyde (NDA) is a fluorogenic reagent designed for the derivatization of primary amines such as carnosine.<sup>23</sup> NDA reacts with primary amines in the presence of cyanide (CN<sup>-</sup>) to produce highly fluorescent 1-cyanobenz[*f*]isoindole (CBI) derivatives. The reaction of carnosine with NDA/CN<sup>-</sup> is shown in Fig. 1. These CBI derivatives have previously been used for the detection of biogenic amines by ME-LIF.<sup>24–26</sup>

The aim of this study was to develop a method for the determination of the intracellular carnosine concentration in murine RAW 264.7 macrophage cells as a function of stimulation protocol. Carnosine and other primary amines present in cell lysates were derivatized with NDA/CN<sup>-</sup> and then separated and detected by ME-LIF. This method was then used to investigate variations in carnosine uptake by macrophages under physiological and pro-inflammatory conditions.

## Materials and methods

### Materials and reagents

Murine RAW 264.7 cells (ATCC® TIB71™), Dulbecco's Modified Eagle's Medium (DMEM), phenol red-free DMEM, fetal bovine serum (FBS), and penicillin/streptomycin antibiotic solution were purchased from American Type Culture Collection (ATCC, Manassas, VA, USA). L-Carnosine, sodium cyanide (NaCN), anhydrous dimethyl sulfoxide (DMSO), phosphate-buffered saline (PBS), trypan blue solution, lipopolysaccharides (LPS), Triton X-100, and bovine serum albumin (BSA) were all supplied by Sigma-Aldrich (St. Louis, MO, USA). Sodium hydroxide (NaOH), hydrochloric acid (HCl), 25 mL polystyrene culture flasks, boric acid, and ethanol (95%) were obtained from Fisher Scientific (Pittsburgh, PA, USA). Interferon- $\gamma$  (IFN- $\gamma$ ) was supplied by Calbiochem (Gibbstown, NJ, USA). Naphthalene-2,3-dicarboxaldehyde (NDA) was obtained from Invitrogen (Carlsbad, CA, USA). Polyethersulfone (PES) membrane (3K) was purchased from VWR International (West Chester, PA, USA). C-Chip disposable hemocytometer was purchased from Bulldog Bio, Inc. (Portsmouth, NH, USA). All water used was Ultrapure (18.3 M $\Omega$  cm) (Milli-Q Synthesis A10, Millipore, Burlington, MA, USA).

### Preparation of carnosine standards, derivatization solutions, and background electrolyte

Carnosine standards were prepared at 0.5 M in water before further dilution. NDA was prepared in acetonitrile at

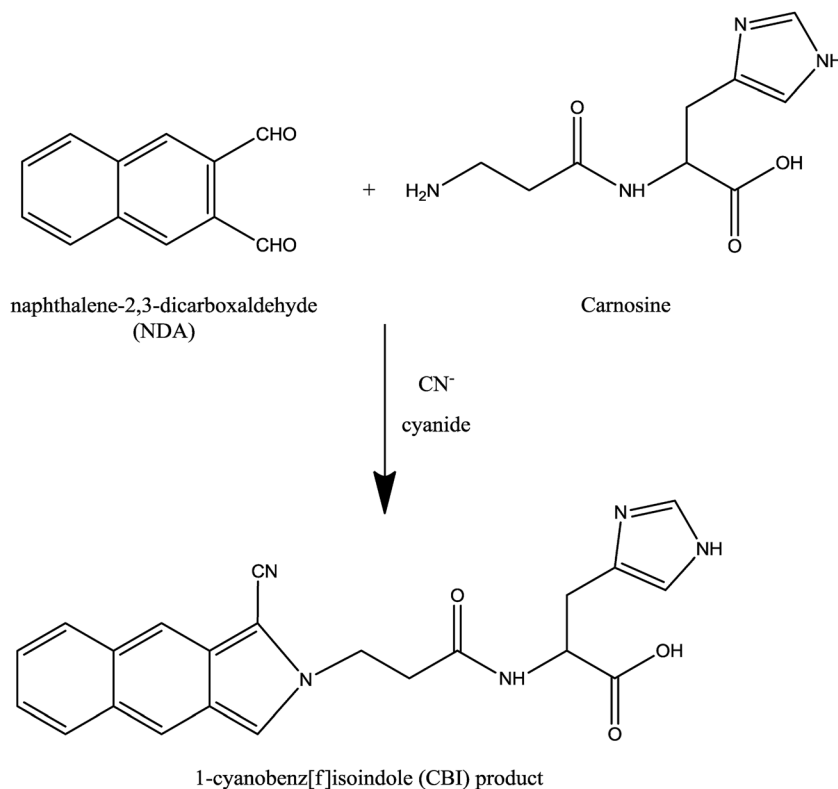


Fig. 1 Derivatization reaction schemes of naphthalene-2,3-carboxaldehyde (NDA) and carnosine in the presence of cyanide (CN<sup>-</sup>).

a concentration of 5 mM, while NaCN was dissolved in water at a concentration of 10 mM. Fresh solutions of NaCN, NDA, and carnosine were prepared weekly, stored at 4 °C (−20 °C for carnosine), and protected from light exposure. The sodium borate background electrolyte (BGE) was prepared from 20 mM boric acid titrated to pH 9.2 *via* the addition of 0.1 M NaOH.

### Cell culture and treatment protocol

RAW 264.7 macrophage cells were cultured in DMEM containing 10% (v/v) FBS, L-glutamine (2 mM), penicillin (50 IU mL<sup>−1</sup>), and streptomycin (0.3 mg mL<sup>−1</sup>). The cells were maintained in a humidified environment at 37 °C and 5% CO<sub>2</sub> and cultured in 25 mL polystyrene culture flasks. Cells were passaged every 2–3 days at approximately 90% confluence to avoid overgrowth. On the day of the experiment, cells were harvested, counted, and plated at the density of  $1.5 \times 10^7$  cells per flask. They were then placed in an incubator under a humidified environment at 37 °C and 5% CO<sub>2</sub>. Once the cells adhered to the flask surface they were then stimulated with LPS (100 ng mL<sup>−1</sup>) and INF- $\gamma$  (600 U mL<sup>−1</sup>). After 4 h of stimulation, carnosine (at a final concentration of 20 mM) was added to the cell medium, and the cells were left to incubate for an additional 20 h. For the control experiments, RAW 264.7 cells from the same population were incubated with only 20 mM carnosine (no preincubation with stimulation agents). Additionally, untreated (native) RAW 264.7 cells were analyzed to estimate the basal carnosine concentration. At the end of incubation the cells were harvested using a cell scraper, and the cell suspension was transferred to a centrifuge tube (15 mL). A 100  $\mu$ L aliquot of the solution containing macrophage cells was taken out and cells counted. The cells were then centrifuged at  $1137 \times g$  for 4 min at 4 °C. After centrifugation, the supernatant was removed and the cell pellet was washed twice using cold 0.01 M PBS at pH 7.4. Next, cell pellets were lysed using 300  $\mu$ L of 10 mM boric acid and 0.5% Triton X-100 at pH 9.2. The lysate solution was filtered by centrifugation at  $18\,690 \times g$  for 10 min in centrifuge tubes equipped with 3 kDa cut-off filters. The filtered lysates were then ready for the NDA/CN derivatization procedure. Prior to ME-LIF analysis, each sample lysate (except the native one) was diluted by a factor of 20 in BGE. Cell density and viability were measured as described by de Campos *et al.*<sup>16</sup>

### NDA-CN derivatization reaction

Standards and cell samples were derivatized with NDA/CN. For standards, the appropriate volume of 0.5 M carnosine was diluted with BGE to 1540  $\mu$ L to achieve the desired final concentration. Thirty microliters of 5 mM NDA and 30  $\mu$ L of 10 mM NaCN were then sequentially added with mixing to the vial. For cell samples, 40  $\mu$ L of filtered lysate was diluted with 100  $\mu$ L of BGE before the addition of NDA and NaCN at the same concentrations and volumes.

For the standard addition experiments, the volume of all of the reaction components described above was divided in half so that more aliquots could be analyzed. To determine the basal concentration, 20  $\mu$ L of native cell lysate was divided into four portions. The appropriate volume of the 100  $\mu$ M carnosine standard was added to the lysates to generate standard addition

final concentrations of 1, 2.5, and 5  $\mu$ M carnosine. The samples were diluted with BGE to a total final volume of 70  $\mu$ L before the addition of 15  $\mu$ L of NDA and 15  $\mu$ L of NaCN at the previously mentioned concentrations.

For all experiments, the NDA/CN-derivatization reaction was allowed to proceed for at least 30 min at room temperature, but no longer than 2 hours (CBI derivatives have previously been shown to be stable for up to 10 hours), and protected from light.<sup>23</sup>

### Microchip electrophoresis with laser-induced fluorescence (ME-LIF)

The fabrication of glass microfluidic devices using photolithographic techniques has been described previously.<sup>25</sup> The design used in these experiments included a 15 cm serpentine separation channel with 3 cm side channels and a 1.5 cm injection channel. These channels were approximately 17  $\mu$ m deep and 70  $\mu$ m wide. Prior to use, the microchip was conditioned with 0.1 M HCl, deionized water, 0.1 NaOH, and deionized water. Each solution was allowed to flow through the channels for approximately 10 min by the application of negative pressure using a vacuum system. The channels were then filled with BGE by the same process.

Separations were performed in normal polarity using a high voltage power supply (Ultravolt, Ronkonkoma, NY, USA) controlled by software written in Labview (National Instruments, Austin, TX, USA). For separations, 10 kV was applied to the buffer reservoir and 7 kV to the sample reservoir, resulting in a field strength of 420 V cm<sup>−1</sup> and an analysis time of 150 s (2.5 min). Electrokinetic injections were employed by floating the buffer reservoir voltage for 0.5 s to produce a sample plug. The channels were re-conditioned between each cell lysate sample to remove any residual CBI products and cellular debris.

The benchtop ME-LIF system used for these experiments has been described previously.<sup>24</sup> Briefly, a 445 nm PhoxX diode laser (Market Tech, Scotts Valley, CA, USA) was coupled to an Eclipse Ti-U inverted microscope (Nikon Instruments Inc., Melville, NY, USA) *via* a fiber optics cable. As CBI derivatives have an emission maximum of 490 nm,<sup>23</sup> the emission light was filtered through a long-pass edge filter with a 480 nm cutoff before being focused onto a photomultiplier tube (Hamamatsu Corporation, Bridgewater, NJ, USA). The resulting data were amplified and filtered before acquisition using Labview software. Data analysis was performed using Origin 8.2 software (OriginLab, Northampton, MA, USA).

### Cell imaging

Cell images were obtained using an Accu-Scope microscope (Mel Sobel Microscopes Ltd, Hicksville, NY, USA) with Micro-Publisher 3.3 RTV camera (Qimaging, Surrey, BC, Canada), while QCapture Pro 6 software (Qimaging) was employed for image analysis.

### Statistical analysis

Normal data distribution was determined using the Kolmogorov–Smirnov test. The within-group comparison was performed by one-way analysis of variance (ANOVA). Differences across groups were estimated by two-way ANOVA. Fisher's Protected Least Squares Differences was used as the post hoc test.

## Results and discussion

### Identification and quantification of carnosine in untreated cultured macrophages

The first aim of this study was to determine if RAW 264.7 murine macrophage cells naturally contain carnosine under normal physiological conditions. A separation of carnosine from the most abundant amino acids reported to be in macrophage cells was developed using standards.<sup>27</sup> The separation employed an all-glass 15 cm glass microchip with a BGE of 20 mM sodium borate (pH 9.2) and a field strength of  $420 \text{ V cm}^{-1}$ . None of the abundant amino acids co-migrated with carnosine under these optimal separation conditions (Fig. 2A). Fig. 2B shows an electropherogram of an untreated macrophage cell lysate obtained following NDA/CN derivatization; it contains many peaks due to the presence of these constituent primary amines, including a peak co-migrating with the carnosine standard (Fig. 2C). As can be seen in this Fig. 2, there was a shift in the migration time of carnosine for the cell lysate sample compared to that for the standard solution. This shift is due to the higher conductivity of the lysate samples compared to that of the standards. During the lysis process, intracellular ions are released into the lysis buffer leading to

a substantial increase in the ionic strength of the sample. It has been documented that high conductivity sample plugs can result in longer migration times for electrophoretic separations.<sup>28</sup>

Using carnosine standards, a calibration curve was constructed over a concentration range of 25 nM to 1  $\mu\text{M}$ . The system displayed good linearity, with a correlation coefficient ( $R^2$ ) of 0.994. The experimentally determined limit of detection (LOD) for carnosine was 65 nM ( $S/N = 3$ ). This LOD was sufficient for the measurement of physiologically relevant concentrations of carnosine. The migration time of the CBI-carnosine peak exhibited a relative standard deviation of 3.55%.

Assuming that the peak that co-migrated with added carnosine is the authentic compound, the carnosine content in native (control) cell lysates was determined using the method of standard additions (Fig. 3). The standard addition of response vs. carnosine concentration added yielded a  $R^2$  value of 0.997. Using the cell counts obtained for each set of untreated cells, the concentration of carnosine contained per million of cells could be determined, with a calculated concentration of  $0.079 \pm 0.02 \text{ nmol per } 10^6 \text{ cells}$ . Macrophage cells are known to be the first immunocompetent cells to respond to different inflammation processes,<sup>14</sup> such as oxidative stress. Therefore, the

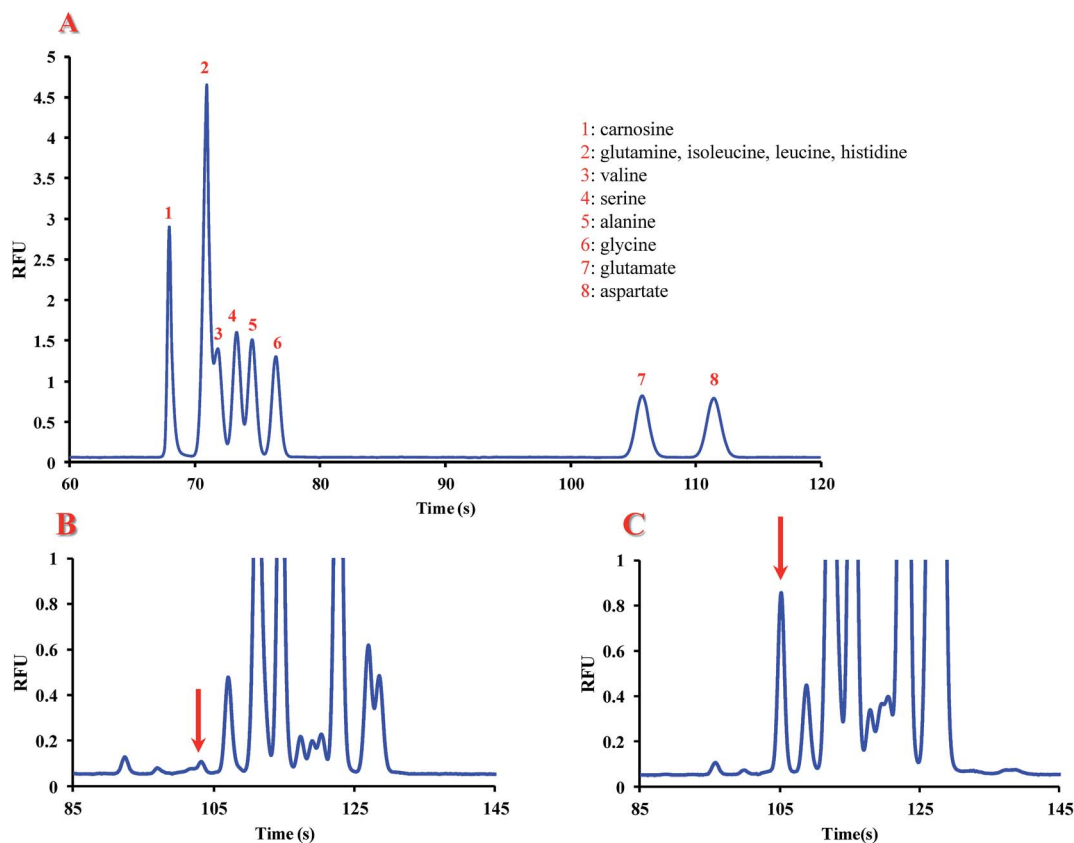


Fig. 2 (A) Electropherogram showing the separation of carnosine from endogenous intracellular amino acids by microchip CE using an all-glass 15 cm glass microchip, a BGE of 20 mM borate at pH 9.2, and a field strength of  $420 \text{ V cm}^{-1}$ . All standards are at concentrations of 5  $\mu\text{M}$ . (1) Carnosine; (2) histidine, glutamine, isoleucine, leucine; (3) valine; (4) serine; (5) alanine; (6) glycine; (7) glutamate; (8) aspartate. (B) Representative electropherogram of a untreated macrophage cell lysate. The putative peak corresponding to carnosine was identified based on its migration time and confirmed *via* spiking with standards (C). Carnosine peaks are indicated with red arrows.

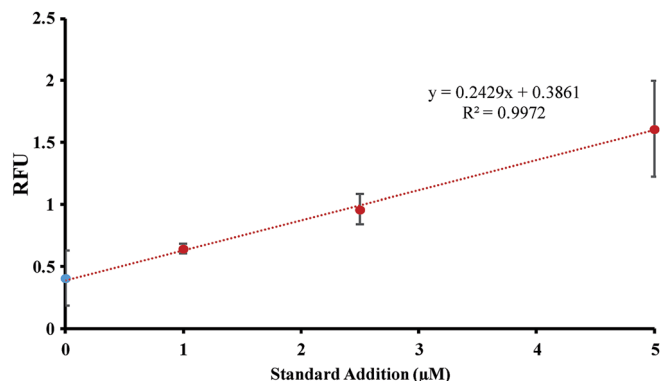


Fig. 3 Standard addition calibration curve of carnosine in native cell lysate.

presence of a basal amount of carnosine in these immune cells under physiological conditions could be related to its antioxidant activity in counteracting oxidative stress by scavenging RNOS.<sup>6</sup> Future work will confirm the presence of carnosine in the native cell lysate using LC-MS.

#### Comparison of carnosine uptake in different stimulated cultured macrophages using ME-LIF

The toxic effects of cellular pro-oxidants can be mitigated by the presence of antioxidant molecules<sup>29,30</sup> such as carnosine.<sup>6</sup> This pro-oxidant/antioxidant balance is important for regulating cellular nitrosative stress<sup>31</sup> and is connected to cell death.<sup>32</sup> The second aim of this study was to investigate the variation in carnosine uptake by RAW 264.7 macrophages under physiological and pro-inflammatory conditions. This will provide a better understanding of carnosine's protective role during

macrophage activation caused by pro-inflammatory agents such as LPS and IFN- $\gamma$ .

Carnosine is taken up by macrophages if it is placed in the cell medium. In these studies, we wanted to determine the effect of inflammation on carnosine uptake. This was accomplished by incubating the macrophages with LPS + IFN- $\gamma$  4 h prior to incubation with 20 mM carnosine. These results were then compared to control experiments, where the cells were incubated with only carnosine. The protocol for the determination of intracellular carnosine using cell lysates is shown in Fig. 4A. The effect of carnosine on macrophage morphology under the two different conditions is shown in Fig. 4B. The addition of carnosine alone to the cell medium did not affect the cell morphology (Fig. 4BI). On the other hand, pronounced differentiation was observed following treatment of RAW 264.7 cells with a combination of LPS, IFN- $\gamma$ , and then carnosine (Fig. 4BII). The latter cells exhibited a large increase in the number of cellular processes, which is indicative of differentiated and activated macrophages.

Fig. 5A shows typical electropherograms for cells incubated with carnosine alone (20 mM) and cells stimulated with LPS + IFN- $\gamma$  prior to incubation with carnosine (20 mM). There was a noticeable shift in the migration times between the samples, which was assumed to be due to the previously mentioned conductivity differences in the sample matrix. Therefore, all cell samples were spiked with carnosine standards in order to confirm the peak identity. Due to the large amount of carnosine present within the incubated cells compared to the native cells, a new calibration curve was constructed using a concentration range of 1  $\mu$ M to 50  $\mu$ M ( $R^2 = 0.999$ ). The cell count in each individual sample was once again taken into consideration when calculating the final carnosine concentration. A dramatic increase in carnosine uptake was observed in stimulated

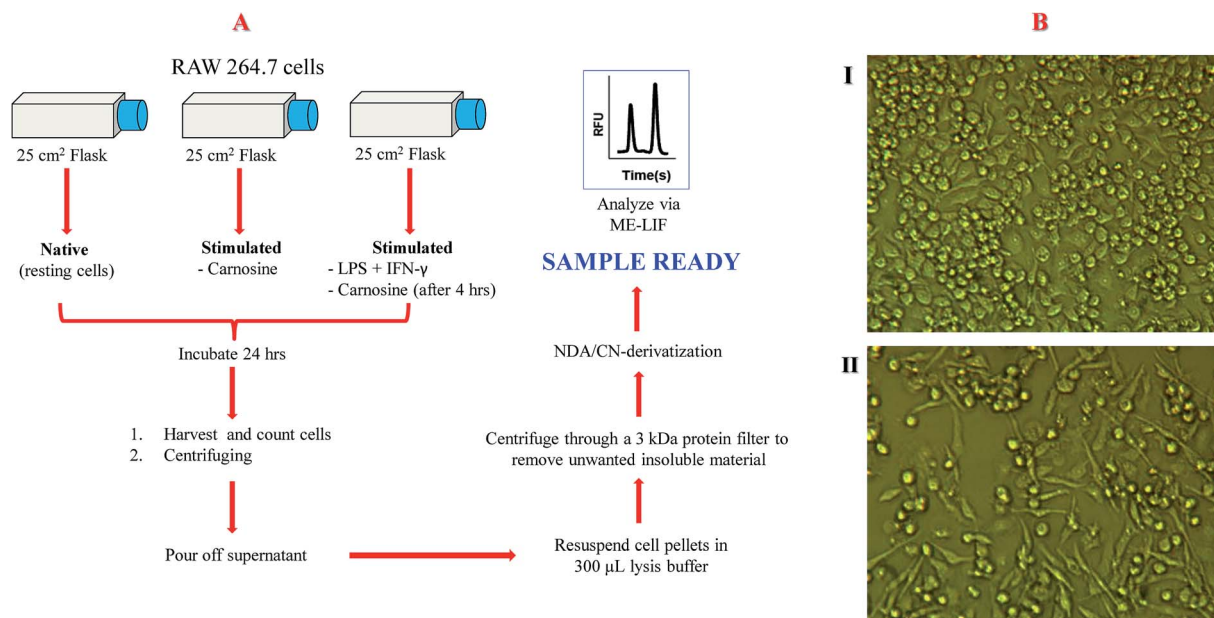


Fig. 4 (A) Diagram of experimental procedure. (B) Morphological changes in murine RAW 264.7 cells following different stimulation protocols: (I) treated with carnosine (20 mM); (II) treated with LPS (100 ng mL<sup>-1</sup>), IFN- $\gamma$  (600 U mL<sup>-1</sup>), and carnosine (20 mM).

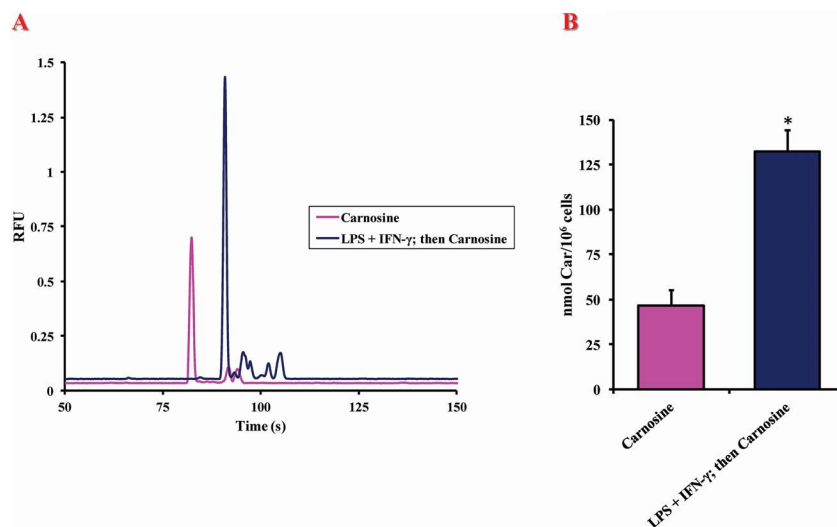


Fig. 5 (A) Representative electropherograms of cell lysates showing the change in peak area of carnosine for macrophages stimulated with carnosine (purple) and stimulated with LPS + IFN- $\gamma$  followed by 20 mM carnosine (dark blue). (B) Graph of intracellular concentrations of carnosine in macrophages stimulated with carnosine and of macrophages stimulated with LPS + IFN- $\gamma$  followed by 20 mM carnosine. Values are the mean of four different experiments. Standard deviations are represented by vertical bars. \*significantly different from cells incubated with carnosine only ( $p < 0.001$ ).

compared to unstimulated cells. Fig. 5B shows bar graphs for the average intracellular content of carnosine under the two different experimental conditions. There was an approximately 2.8-fold increase ( $2.83 \pm 0.29$ ) in carnosine uptake in cells stimulated with LPS + IFN- $\gamma$  and then incubated with 20 mM carnosine ( $132.41 \pm 12.22$  nmol per  $10^6$  cells) vs. cells incubated with carnosine only ( $46.67 \pm 8.61$  nmol per  $10^6$  cells). The calculated intracellular carnosine concentration of a LPS + IFN- $\gamma$ -stimulated cell was statistically significant ( $p < 0.001$ ) compared to that of the control.

The increased uptake in stimulated macrophages could be caused by a number of factors including: (1) macrophages, as a part of immune system, can increase the uptake of antioxidant molecules (carnosine) as a defense mechanism in response to pro-inflammatory stimuli;<sup>33</sup> (2) the presence of stressing agents, such as LPS and IFN- $\gamma$ , can influence cell membrane permeability;<sup>34</sup> and/or (3) increased antioxidant transporter activity<sup>35</sup> as a consequence of cell morphological changes observed after stimulation (Fig. 4B). We plan to investigate each of these potential pathways in the future.

## Conclusions

In this report, a microchip electrophoresis system with fluorescence detection was used for the quantitation of intracellular carnosine in untreated and stimulated macrophage cell lysates. Carnosine was derivatized with NDA/CN and separated from other endogenous amine reported in macrophage cells. Based on ME-LIF with standard addition, macrophages were estimated to contain a basal intracellular concentration of carnosine ( $0.079 \pm 0.02$  nmol per  $10^6$  cells). Carnosine is readily taken up by macrophages in cell culture. Incubation with 20 mM carnosine led to a 600-fold increase in intracellular carnosine

compared to basal levels. Furthermore, we have shown that under pro-inflammatory conditions using LPS and IFN- $\gamma$  stimulation there is a further 3-fold increase in carnosine uptake in macrophage cells. This suggests that there is a mechanism through which macrophages increase the usage of carnosine during oxidative stress. Future studies will focus on determining the mechanism of increased transport and the role of intracellular carnosine in fighting oxidative stress.

## Conflict of interest

The authors have declared no conflict of interest.

## Acknowledgements

This work was performed with financial support from NSF (CHE-1411993), NIH (R01NS042929), COBRE (P20GM103638), and NIH (R01NS066466). GC gratefully acknowledges the support of an American Heart Association-Midwest Affiliate Postdoctoral Research Fellowship (NFP0075515). We would also like to thank Nancy Harmony for editorial support and Nathan Oborny for help with microchip fabrication.

## References

- 1 S. Budzeń and J. Rymaszewska, *Adv. Clin. Exp. Med.*, 2013, **22**, 739–744.
- 2 A. R. Hipkiss, J. E. Preston, D. T. Himsworth, V. C. Worthington, M. Keown, J. Michaelis, J. Lawrence, A. Mateen, L. Allende, P. A. Eagles and N. J. Abbott, *Ann. N. Y. Acad. Sci.*, 1998, **854**, 37–53.
- 3 A. E. Gariballa and A. J. Sinclair, *Age Ageing*, 2000, **29**, 207–210.

- 4 C. A. Hill, R. C. Harris, H. J. Kim, B. D. Harris, C. Sale, L. H. Boobis, C. K. Kim and J. A. Wise, *Amino Acids*, 2007, **32**, 225–233.
- 5 M. A. Kamal, H. Jiang, Y. Hu, R. F. Keep and D. E. Smith, *Am. J. Physiol.: Regul., Integr. Comp. Physiol.*, 2009, **296**, R986–R991.
- 6 A. R. Hipkiss, *Adv. Food Nutr. Res.*, 2009, **57**, 87–154.
- 7 H. L. Hsieh and C. M. Yang, *BioMed Res. Int.*, 2013, **2013**, 484613.
- 8 O. A. Barski, Z. Xie, S. P. Baba, S. D. Sithu, A. Agarwal, J. Cai, A. Bhatnagar and S. Srivastava, *Arterioscler., Thromb., Vasc. Biol.*, 2013, **33**, 1162–1170.
- 9 Y. T. Lee, C. C. Hsu, M. H. Lin, K. S. Liu and M. C. Yin, *Eur. J. Pharmacol.*, 2005, **513**, 145–150.
- 10 A. A. Fouad, M. A. El-Rehany and H. K. Maghraby, *Eur. J. Pharmacol.*, 2007, **572**, 61–68.
- 11 A. A. Boldyrev, G. Aldini and W. Derave, *Physiol. Rev.*, 2013, **93**, 1803–1845.
- 12 A. Guiotto, A. Calderan, P. Ruzza and G. Borin, *Curr. Med. Chem.*, 2005, **12**, 2293–2315.
- 13 M. V. Onufriev, G. I. Potanova, S. A. Silaeva and A. Nikolaev, *Biokhimiya*, 1992, **57**, 1352–1359.
- 14 F. O. Martinez, L. Helming and S. Gordon, *Annu. Rev. Immunol.*, 2009, **27**, 451–483.
- 15 D. S. Chi, M. Qui, G. Krishnaswamy, C. Li and W. Stone, *Nitric Oxide*, 2003, **8**, 127–132.
- 16 R. P. de Campos, J. M. Siegel, C. G. Fresta, G. Caruso, J. A. F. da Silva and S. M. Lunte, *Anal. Bioanal. Chem.*, 2015, **407**, 7003–7012.
- 17 D. B. Gunasekara, J. M. Siegel, G. Caruso, M. K. Hulvey and S. M. Lunte, *Analyst*, 2014, **139**, 3265–3273.
- 18 Z. Chen, Q. Li, Q. Sun, H. Chen, X. Wang, N. Li, M. Yin, Y. Xie, H. Li and B. Tang, *Anal. Chem.*, 2012, **84**, 4687–4694.
- 19 R. A. Hunter, B. J. Privett, W. H. Henley, E. R. Breed, Z. Liang, R. Mittal, B. P. Yoseph, J. E. McDunn, E. M. Burd, C. M. Coopersmith, J. M. Ramsey and M. H. Schoenfisch, *Anal. Chem.*, 2013, **85**, 6066–6072.
- 20 E. R. Mainz, D. B. Gunasekara, G. Caruso, D. T. Jensen, M. K. Hulvey, J. A. F. da Silva, E. C. Metto, A. H. Culbertson, C. T. Culbertson and S. M. Lunte, *Anal. Methods*, 2012, **4**, 414–420.
- 21 N. Nuchtavorn, W. Suntornsuk, S. M. Lunte and L. Suntornsuk, *J. Pharm. Biomed. Anal.*, 2015, **113**, 72–96.
- 22 C. Bylda, R. Thiele, U. Kobold and D. A. Volmer, *Analyst*, 2014, **139**, 2265–2276.
- 23 P. De Montigny, J. F. Stobaugh, R. S. Givens, R. G. Carlson, K. Srinivasachar, L. A. Sternson and T. Higuchi, *Anal. Chem.*, 1987, **8**, 96–101.
- 24 N. J. Oborny, E. E. Costa, L. Suntornsuk, F. C. Abreu and S. M. Lunte, *Anal. Sci.*, 2016, **32**, 35–40.
- 25 T. H. Linz, C. M. Snyder and S. M. Lunte, *J. Lab. Autom.*, 2012, **17**, 24–31.
- 26 P. Nandi, D. E. Scott, D. Desai and S. M. Lunte, *Electrophoresis*, 2013, **34**, 895–902.
- 27 H. Sato, H. Watanabe, T. Ishii and S. Bannai, *J. Biol. Chem.*, 1987, **262**, 13015–13019.
- 28 Z. K. Shihabi, *Handbook of Capillary Electrophoresis*, ed. J. P. Landers, CRC Press, 2nd edn, 1997, pp. 457–477.
- 29 M. Valko, D. Leibfritz, J. Moncol, M. T. Cronin, M. Mazur and J. Telser, *Int. J. Biochem. Cell Biol.*, 2007, **39**, 44–84.
- 30 H. Zhang and H. J. Forman, *Semin. Cell Dev. Biol.*, 2012, **23**, 722–728.
- 31 J. B. Schulz, J. Lindenau, J. Seyfried and J. Dichgans, *Eur. J. Biochem.*, 2000, **267**, 4904–4911.
- 32 Z. V. Varga, Z. Giricz, L. Liaudet, G. Haskó, P. Ferdinandy and P. Pacher, *Biochim. Biophys. Acta*, 2015, **1852**, 232–242.
- 33 M. A. Puertollano, E. Puertollano, G. Á. de Cienfuegos and M. A. de Pablo, *Curr. Top. Med. Chem.*, 2011, **11**, 1752–1766.
- 34 C. T. Capaldo and A. Nusrat, *Biochim. Biophys. Acta*, 2009, **1788**, 864–871.
- 35 D. Sun, Y. Wang, F. Tan, D. Fang, Y. Hu, D. E. Smith and H. Jiang, *Mol. Pharm.*, 2013, **10**, 1409–1416.